ELSEVIER

Biophysical Chemistry 91 (2001) 141–155

Biophysical Chemistry

www.elsevier.nl/locate/bpc

Study of human serum albumin-TiO_2 nanocrystalline electrodes interaction by impedance electrochemical spectroscopy

Fabiana Y. Oliva*, Lucía B. Avalle, Vicente A. Macagno, Carlos P. De Pauli

INFIQC, Departamento de Fisicoquímica, Facultad de Ciencias Químicas, Universidad Nacional de Córdoba, Ciudad Universitaria, Córdoba 5000, Argentina

Received 16 October 2000; received in revised form 9 April 2001; accepted 11 April 2001

Abstract

The adsorption of human serum albumin (HSA) onto nanocrystalline TiO_2 electrodes was studied by electrochemical impedance spectroscopy (EIS) in function of pH and electrode potential. The characterization and physico-chemical properties of the TiO_2 electrode were investigated by scanning electron microscopy (SEM), UV-photoelectron spectroscopy (UPS), cyclic voltammetry and capacitance measurements. The impedance response of the particulate TiO_2 electrode/protein interface was fitted using an equivalent circuit model to describe the adsorption process. The adsorbed protein layer, which is formed as soon as the protein is injected into the solution and becomes in contact with the electrode, was investigated as a function of electrode potential and solution pH. The measurements were performed under pseudo-steady-state and steady-state conditions, which gave information about the different states of the system. With the pseudo-steady state measurements, it was possible to determine two rate constants of the protein adsorption process, which correspond to two different states of the protein. The shortest one was associated with the first contact between the protein and the substrate and the second relaxation time, with the protein suffering an structural rearrangement due to the interaction with the TiO_2 electrode. It was detected that at sufficiently long times (approx. 1 h, where the system was under steady state conditions), a quasi-reversible protein adsorption mechanism was established. The measurements performed as a function of frequency under steady-state conditions, an equivalent circuit with a Warburg element gave the better fitting to data taken at -0.585 V closer to the oxide flat band potential and it was associated with protein diffusion. Experimental results obtained at only one frequency as a function of potential could be fitted to a model that takes into account non-specific and probable

* Corresponding author. Tel.: +54-51-334169; fax: +54-51-334188.
E-mail address: foliva@fisquim.fcq.unc.edu.ar (F.Y. Oliva).

PII: S0301-4622(01)00166-1

specific protein adsorption, which renders to be potential- and pH-dependent. Low capacity values were obtained in the whole potential range, which were measured in the presence and in the absence of the protein layer. The capacity dependence on potential and pH were associated with the generation of surface states on TiO_2. A surface state concentration of 4.1×10^{18} cm^{-2} was obtained by relating the parallel capacitance with oxide surface states arising from the protein–oxide interaction.

Keywords: Human serum albumin; TiO_2 nanocrystalline; Adsorption mechanism; Surface states

1. Introduction

The practical importance of TiO_2 lies in its wide field of applications. The optical and electrical properties of TiO_2 have applications in gas-sensing devices, photochemical energy conversion processes [1], antireflection coatings and fabrication of oxidase — based biosensors [2,3]. In addition, its use as a biocompatible material raises questions about whether surfaces cause biomolecules to denature, whether the optimum length of linking groups and ways to interact from the biomolecule, through the linker, to the substrate [4].

The TiO_2/electrolyte interface has been tested for a great variety of titanium-dioxide materials and its crystallographic states (polycrystalline anatase or rutile or single-crystal rutile) have been characterized, demonstrating that the physicochemical properties of TiO_2 are determined by its chemical origin and different preparation methods. Oxide layers can be prepared by different ways, e.g. thermal [5] or electrochemical oxidation of metallic titanium [6] or by sol–gel deposition as in our case [7].

The most striking feature of the semiconductor particulate films is the ability to retain the properties of individual semiconductor particles and thus carry out the reactions with similar selectivity and efficiency as in semiconductor particle suspensions. Such a film provides a convenient way of manipulating the protein adsorption by electrochemical methods. If one can drive the electric charges on the sorbent surface (by changing the electrode potential), independent of solution pH, it should be possible to follow the protein adsorption when charge signs on the protein and the TiO_2 are similar or opposed. But whether they prevent adsorption or not, it also depends on other factors such as dehydration of the protein and the sorbent as well as on structural rearrangements in the protein molecule. Human serum albumin (HSA), on the other hand, adsorbs at any interface even if the sorbent is hydrophilic and has the same charge sign as the protein. In this case, the driving force for adsorption stems from dehydration and/or conformational changes in the protein molecule [8]. Although a same charge sign may not prevent adsorption, it may slow down the process [4].

There are many studies about protein adsorption on different electrodes, mainly metals [9,10], but there is very little information regarding protein-semiconductor electrodes using electrochemical impedance spectroscopy. Thus, we investigated the electric behavior of the TiO_2 interface in the presence and absence of the protein.

In this work we have determined the HSA adsorption mechanism onto nanocrystalline TiO_2 electrodes by employing the impedance method. Kinetic rate constants of the adsorption process were determined by pseudo-steady state measurements and for a long time (stationary conditions), a quasi-reversible behavior was postulated and a physical model that considers generation of oxide surface states due to protein adsorption is taken into account. Calculations about this process are adjusted to experimental data.

2. Experimental

2.1. Materials

2.1.1. Chemicals

The measurements were performed in 0.1 M NaCl solutions, where the protein does not un-

dergo any changes at this ionic strength and the high salt concentration is adequate to decrease electrolyte resistance to perform electrochemical measurements. The pH of the solution was adjusted either with HCl or NaOH before each experiment and checked with an Orion 960 autochemistry system. Although this solution is not a buffer, no significant variations in the solution pH were observed during the experiment. The working pH effect was analyzed in a range of approximately 2 units around the protein isoelectric point (IEP) (i.e. 4.7). The HSA (fraction V) was provided by Laboratorio de Hemoderivados, Universidad Nacional de Córdoba (Argentina) and used without further purification. The protein concentration was determined spectrophotometrically in an UV 1601 Shimadzu spectrophotometer at 279 nm. All the solutions as well as glassware cleaning were performed with water Milli-Q Millipore System. Different aliquots of a stock protein solution were injected to 50-ml 0.1 M NaCl to give various final protein concentrations in the electrochemical cell. All chemicals were of analytical grade and purchased from MERCK used without further purification.

2.1.2. Cells and electrodes

A three-electrode system was used for all experiments under N_2 atmosphere at room temperature. The counter electrode was a platinum electrode with a large area and the reference electrode was a double junction saturated calomel electrode (SCE).

The working electrode was a Ti/TiO_2 nanocrystalline. Cathodic electrodeposition of nanocrystalline titanium dioxide film onto titanium electrodes was carried out as described elsewhere [7]. The substrate, a titanium rod that was mechanically polished until 1 μm with alumina was cleaned with $HF/HNO_3/H_2O$, 1:4:5 for 10 s before immersion in the $TiO(NO_3)_2$ deposition bath. The nanocrystallite oxide deposition was carried out potentiostatically at −1.1 V for 5 min. This process was performed several times until a certain thickness was obtained. This type of method (with a temperature treatment approx. 400°C) allows formation of the anatase phase of the oxide with a large surface area.

2.2. Methods

2.2.1. SEM and UPS measurements

The surface morphology was observed by scanning electron microscopy (SEM) at high resolution. UV-Photoelectron spectroscopy (UPS) measurements were performed at the Campinas Sincrotron, SP, Brazil in the TGM (Toroidal Grating Monochromator) beam line. The pressure in the sample chamber was in the 10^{-9}-mbar range. In order to obtain information about the composition at different film depths, TiO_2 samples were argon sputter etched (2 KeV, 20 μA) in the preparation chamber for different periods of time.

2.2.2. Cyclic voltammetry measurements

Voltammetric curves were recorded after a stabilization of five cycles between −0.4 and 1.5 V vs. SCE at 100 mV/s starting at the electrode rest potential (approx. −0.185 V vs. SCE) in 0.1 M NaCl. After the voltammograms of the electrode were recorded in 0.1 M NaCl, aliquots of protein were added to the electrochemical cell and the electrochemical measurements were repeated with each aliquot.

2.2.3. Impedance measurements

Two impedance methodologies were used to investigate the adsorption of HSA on TiO_2 particulate electrodes, under pseudo-steady state and steady state conditions. The kinetics of HSA adsorption was determined and the measurements were performed as if the system were under steady state during data acquisition. For each time and at a given frequency, the capacity value is recorded. This value is the average of several measurements taken at 0.5 s where the minimal signal variation takes place.

At long times, approximately 1 h (after protein was added) the recording showed that the capacitance tends to a steady state value, where these conditions were considered as steady state of the adsorbed albumin. The stabilization of the electrode potential at open circuit (ocp) was recorded until a minimal variation (approx. 1 mV) was observed. The electrode potential was fixed to a given value, −0.585 V and 1.40 V, selected to give a different charge in the semiconductor space

charge region. The system was polarized to the selected potentials as long as it was necessary to reach almost constant current values (changes approx. 0.1 μA) for approximately 1 h. The impedance measurements were performed after a steady state current or potential value was achieved. This procedure was carried out before and after a protein amount was added into the bulk solution.

The amplitude of the a.c. perturbation signal was 10 mV superimposed on a d.c. potential using a ZANHER IM5D analyzer.

2.2.3.1. Impedance measurements performed at constant potential and frequency: pseudo-steady state conditions. Employing a circuit R(RC) as shown in Fig. 1, the total impedance value is given by:

$$Z_{(\omega)} = R_s + \frac{R_p}{1 + R_p^2 C_T^2 \omega^2} - j\frac{R_p^2 C_T^2 \omega}{1 + R_p^2 C_T^2 \omega^2} = a + jb \quad (1)$$

where ω is the angle frequency, R_p is the parallel resistance and a and b are the real and imaginary parts of impedance, respectively. For high enough values of ω, $R_p^2 C_T^2 \omega^2 \gg 1$ and $b = 1/(C_T \omega)$ so that changes in the imaginary part of the impedance reflect the changes in the total capacity of the system C_T at a given frequency.

We will assume that the main contribution to changes in capacity after protein addition is given by surface localized states generated in the oxide by the interaction with the protein. Nevertheless, a general approach will be presented and the contribution of the Helmholtz capacity C_H, surface states capacity C_{ss} and space charge layer capacity of the semiconductor C_{sc} to the total capacity must be considered:

$$\frac{1}{C_T} = \frac{1}{C_H} + \frac{1}{C_{ss} + C_{sc}}. \quad (2)$$

The impedance measurements were performed at 18 and 80 Hz in a range where the capacity is independent of the frequency (Fig. 1) and the experimental noise from the electric line is minimal because it is outside the resonance frequency

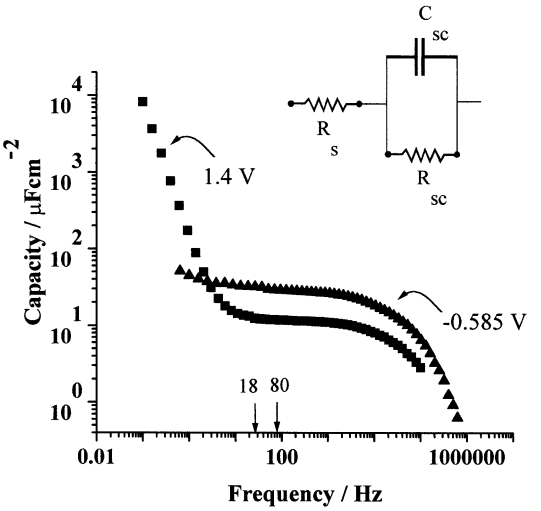

Fig. 1. Electrode capacity vs. log (frequency) plot, in 0.1 M NaCl at two potential values, pH 4.7 and room temperature. The arrows show 18- and 80-Hz frequencies. The capacity was calculated from the equivalent circuit shown in this figure, which is referred as R(RC) notation in the text.

(50 Hz) and its harmonics. Fig. 1 shows $1/\omega Z_{imag} \approx$ total capacity vs. f recorded for the system. A plateau can be seen between 5 and 1200 Hz where the capacity remains almost independent of the frequency. The measurements were performed at constant potential (−0.585 and 1.4 V) in NaCl 0.1 M at pH 4.7.

2.2.3.2. Impedance measurements (EIS) performed at constant potential from 0.1 to 5×10^3-Hz frequency range: steady state conditions. The interface was polarized at −0.585 and 1.40 V. The system was allowed to stabilize at these potentials for 1 h in the presence of 50-ml 0.1 M NaCl at room temperature. During this time, several measurements were recorded in order to evaluate the response of TiO_2 nanocrystalline electrode/electrolyte interface without protein. Then, an aliquot of albumin solution was added, so that the final protein concentration was 0.1 g l^{-1} at pH 4.7. After 1 h of stabilization (when protein was present), the impedance spectrum was recorded. This procedure was repeated at 3.0, 3.6, 7.7 and 8.5 pH values.

The impedance $Z(\omega)$ were displayed in a com-

plex plane over a whole frequency range, forming a parametric curve with ω in which, by convention in electrochemistry, a capacitive feature is characterized by $-Z_{imag}$ and an inductive impedance by $+Z_{imag}$ (Nyquist diagram). From these diagrams, an equivalent circuit was proposed and associated to an appropriate physical model of the system. The elements used in the different equivalent circuits were fitted by the CNLS method (a complex non-linear least square fit) using a commercially available program (EQUIVCRT). Depending on the determining step of the process that takes place at the electrochemical interface, a specific impedance response of the system will prevail. It was, therefore, necessary to adjust the system using different circuits depending on the pH of the solution and electrode potential at which adsorption takes place. Comparison of the experimental diagram with a theoretical diagram calculated on the basis of that assumed equivalent circuit allows one to test the validity of the circuit. Therefore, comparison of the diagrams recorded in the presence of protein with those recorded in its absence should give information on the protein adsorption mechanism.

2.2.3.3. Impedance measurements performed at constant frequency in a potential range from −0.8 to 1.5 V: steady state conditions. The capacity and resistance values were calculated from impedance data using the equivalent circuit shown in Fig. 1 using the $Z(\omega)$ function from Eq. (1). Capacity measurements were performed between −0.8 and 1.5 V at 18 and 80 Hz at different solution pH values of 3.0, 3.6, 4.7, 7.7 and 8.5. At these frequencies the capacity values are almost constant as it is shown in Fig. 1.

3. Results and discussion

3.1. Characterization of nanocrystalline TiO_2 electrodes

Fig. 2 shows a microphotograph obtained for a nanocrystalline TiO_2 electrode. A regular distribution of spherical nanosized particles (≈ 20 nm) can be observed so that the surface area gives an electrode high roughness factor of ≈ 450. The porous semiconductor films [7] were employed and treated in such a way that an anatase structure with a greater area in contact with the electrolyte, resembling semiconductor particle suspensions are obtained.

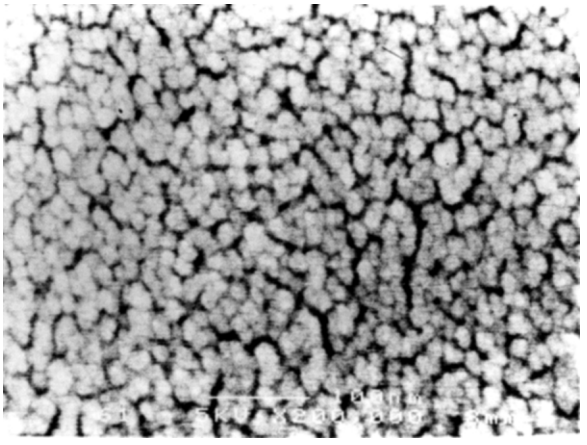

Fig. 2. Microphotograph of the nanocrystalline Ti/TiO_2 electrode obtained by SEM. The mark (——) corresponds to a scale of 100 nm.

In order to get the titanium oxidation state into the oxide net, UPS analysis was performed. Fig. 3 shows UPS spectra at different sputtering times, obtained at the binding energy E_b ranges where the signals corresponding to valence band energy, O2s and Ti3p, are expected to appear. The peak shape corresponding to the valence band changes for different sputtering times. The Ti peak at 37 eV coincides with the values corresponding to Ti^{4+} for the oxide. After a few seconds of sputtering a shoulder appears at smaller values of E_b, indicating the presence of a lower oxidation state, probably Ti^{3+}, whose contribution becomes more significant for deeper oxide layers. However, these experimental facts may not be highly conclusive, because a preferential sputtering of oxygen could produce the reduction of TiO_2. However, the Ti^{3+}/Ti^{4+} redox couple can be observed in the cyclic voltammograms, as it is shown later. For all spectra obtained at different sputtering times, H_2O adsorption could be detected. This bound water layer is proving the film porosity that allows

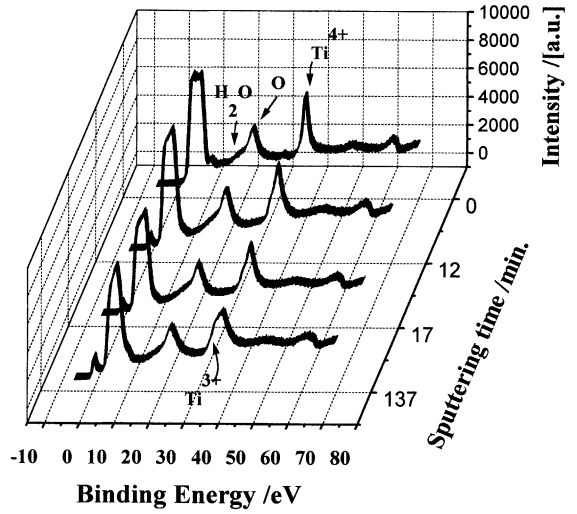

Fig. 3. UPS spectra at different sputtering times with argon ions (2 keV, 20 μA). The O2s peak at 23-eV binding energy was taken as the reference signal.

water to reach the substrate. The TiO_2 nanocrystalline film is deposited onto a titanium substrate, which spontaneously forms a thin oxide layer with n-type semiconductor characteristics. But as it can be seen from Fig. 3, the Ti^{3+} is observed at very superficial layers, indicating that the nanocrystalline film should present n-type semiconductor behavior rather than the behavior presented by small size particles where an appreciable electric field cannot build up in the colloidal film. This may be due to the way that the film is prepared compared with the synthesis developed by other authors [11].

3.2. Dependence of the current–potential curves with the protein concentration

Fig. 4 shows the potentiodynamic current/potential profiles for nanocrystalline TiO_2 electrodes in 0.1 M NaCl pH 4.7 and after the addition of different amounts of protein. In the potential range studied, the hydrogen adsorption–desorption process is also taking place. According to previous results [12], the peak observed during the negative sweep corresponds to Ti(IV) reduction and is related to Ti(III) oxidation during the positive scan which could be expressed as:

$$Ti(OH)^{2+} + H_2O \leftrightarrow [Ti(OH)_2]^{2+} + H^+ + e^- . \quad (3)$$

From 0.02 to 0.1 g l^{-1} HSA, a current decrease is observed compared with the current obtained without protein. This suggests that unsaturated surface Ti^{4+} might be interacting with the protein generating surface states and thus decreasing the Ti^{3+} concentration during the positive potential sweep. However, a clear correlation with HSA concentration cannot be observed, indicating that this methodology cannot be employed to analyze the adsorption process at different coverage degrees. Hereafter, a concentration of 0.1 g l^{-1} was used in all determinations, where the greatest changes were observed.

3.3. Kinetics of HSA adsorption

The experimental data were analyzed by the least-squares non-linear method with a theoretical expression that relate C_T with time and corre-

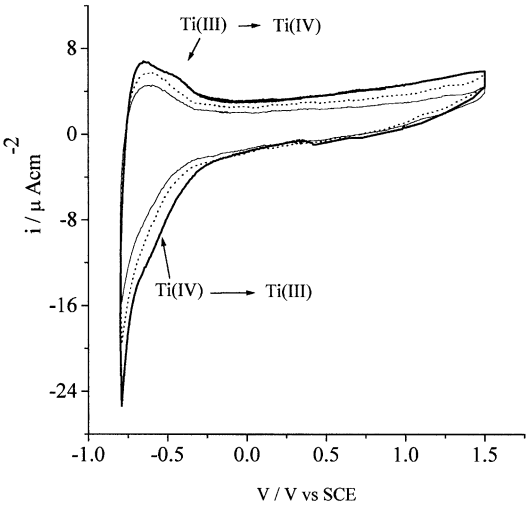

Fig. 4. Cyclic voltammograms for a Ti/TiO_2 electrode in 0.1 M NaCl, pH 4.7 (—) and for different amounts of protein: 0.050 g l^{-1} (---) and 0.1 g l^{-1} (—). Protein was injected at −0.585 V and voltammograms obtained after 1 h of stabilization.

sponds to the sum of the exponential functions of the form:

$$C_T(t) = a_0 + \sum_i a_i e^{-t/\tau_i} \quad (4)$$

where the a_0 and a_i parameters will be later discussed. The fitting yielded two time constants, which suggest that the adsorption is consistent with a two-consecutive step mechanism.

Fig. 5 shows the capacity–time curve, which represents the kinetics of adsorption of the albumin on the electrode. The two consecutive reactions occurring at the interface can be considered as follows:

$$P_{sol} \overset{k_1}{\rightarrow} P_{ads1} \overset{k_2}{\rightarrow} P_{ads2} \quad (5)$$

where P_{sol} refers to the protein in the electrolyte and P_{ads1}, P_{ads2} are two different states of the irreversibly adsorbed protein. A similar mechanism was reported in Pt and glass C rotating disk electrodes with bovine serum albumin (BSA) [13,14]. This physical situation is schematized in Fig. 6.

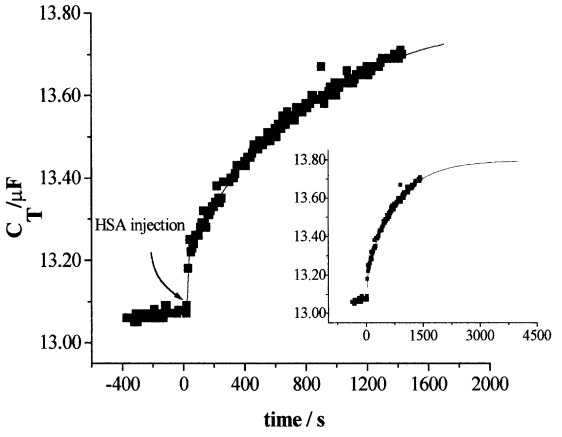

Fig. 5. Time-dependence of the capacity C_T (■) after HSA addition, 0.1 M NaCl, pH 4.7, at −0.585V. Fitted curve (—) was obtained on the basis of the Eq. (4). Parameters obtained from the fitting are shown in the text. The protein injection was considered as $t = 0$ and the capacity variation was recorded for half an hour. Inset shows simulation obtained using the same equation after 1 h of protein injection, $f = 80$ Hz. The results obtained at 18 Hz show the same behavior.

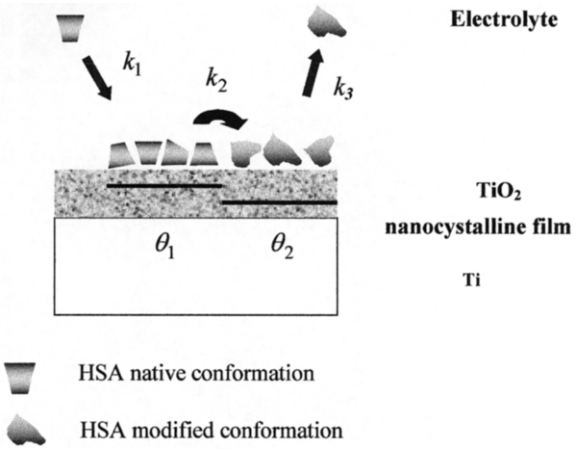

Fig. 6. Scheme of the TiO_2/HSA system in 0.1 M NaCl showing the different steps from protein injection until stationary conditions are established. The changing shape of the protein simulates possible structural rearrangements after adsorption occurs.

The first adsorption step that corresponds to the first relaxation time occurs during the initial 8 s upon contact of the protein with the electrode and thus an adsorption layer is formed (step 1) with a coated electrode fraction θ_1. Afterwards there is a second step in which the protein undergoes a surface rearrangement with τ of 15 min (step 2) with a coating of θ_2. These are consecutive and irreversible first-order steps. The second step can be associated to a modification in the structure of the adsorbed layer or with the adsorption–desorption of a second layer of the protein. The rate equations for these consecutive first-order steps give information about the overall process so they are described below.

The protein initially in solution, P_{sol}, adsorbs to the electrode surface where the initial adsorbed state, P_{ads1}, increases with concentration of the protein in solution, in an apparently first order process, as well as on changing its structure and in a consecutive step, forms another layer of protein adsorbed called P_{ads2}, so that:

$$\frac{d[P_{ads1}]}{dt} = k_1[P_{sol}] - k_2[P_{ads1}]. \quad (6)$$

Finally, this protein restructures and in its final

state is formed at the expense of the protein initially adsorbed:

$$\frac{d[P_{ads2}]}{dt} = k_2[P_{ads1}]. \quad (7)$$

Assuming that the only source of the protein is in solution and its initial concentration is $[P]_0$, and taking into account that this is a first-order process, the albumin concentration in solution undergoes the following variation:

$$[P_{sol}]_t = [P]_0 e^{(-k_1 t)} \quad (8)$$

replacing in Eq. (6) and under the initial condition of $[P_{ads1}]_0 = 0$, $[P_{ads1}]_t$ and $[P_{ads2}]_t$ result in the following:

$$[P_{ads1}]_t = [P]_0 \left\{ \frac{k_1}{k_2 - k_1} \right\} (e^{-k_1 t} - e^{-k_2 t}), \quad (9)$$

$$[P_{ads2}]_t = [P]_0 \left[1 - \frac{k_2}{k_2 - k_1} e^{-k_1 t} + \frac{k_1}{k_2 - k_1} e^{-k_2 t} \right], \quad (10)$$

Considering:

$$[P]_0 = 1$$
$$[P_{ads1}] = \theta_1$$
$$[P_{ads2}] = \theta_2$$

where θ_1 and θ_2 represent the fraction of the electrode covered by the protein in the adsorbed states 1 and 2, respectively. Assuming that the structural changes in the protein occur mainly in the layer that is in contact with the TiO_2 surface, the preceding mentioned processes are in parallel, so that the total capacity of the system will be expressed considering mainly the surface state capacity as it was pointed out in Section 2.2.3.1.

$$C_{ss}(t) = C_{ss0}(1 - \theta_1 - \theta_2) + C_{ss1}\theta_1 + C_{ss2}\theta_2 \quad (11)$$

where C_{ss0}, C_{ss1} and C_{ss2} correspond to the capacity of the oxide surface states without protein and with a monolayer of protein adsorbed in steps 1 and 2, respectively. Thus we obtain the expressions:

$$C_{ss}(t) = C_{ss2} + \left(C_{ss1} \frac{k_1}{k_2 - k_1} - C_{ss2} \frac{k_2}{k_2 - k_1} + C_{ss0} \right) e^{-k_1 t} + \left(C_{ss2} \frac{k_1}{k_2 - k_1} - C_{ss1} \frac{k_1}{k_2 - k_1} \right) e^{-k_2 t} \quad (12)$$

and considering $k_1 = (\tau_1)^{-1}$ and $k_2 = (\tau_2)^{-1}$ we obtain:

$$a_0 = C_{ss2} \quad (13)$$

$$a_1 = C_{ss0} + C_{ss1} \frac{k_1}{k_2 - k_1} - C_{ss2} \frac{k_2}{k_2 - k_1}, \quad (14)$$

$$a_2 = C_{ss2} \frac{k_1}{k_2 - k_1} - C_{ss1} \frac{k_1}{k_2 - k_1}. \quad (15)$$

From the values of the parameters obtained by fitting the experimental data, $a_0 = 13.79\ \mu F$, $a_1 = -1.823\ \mu F$. $\tau_1 = 7.8$ s, $\tau_2 = 814.7$ s, $a_2 = -0.59\ \mu F$, the capacity values are:

- for $\theta_1 = \theta_2 = 0$, $C_{ss0} = 11.39\ \mu F$;
- for $\theta_1 = 1$ and $\theta_2 = 0$, $C_{ss1} = 13.19\ \mu F$; and
- for $\theta_1 = 0$ and $\theta_2 = 1$, $C_{ss2} = 13.80\ \mu F$,

this represents an ideal situation, but during the adsorption process co-exist the two states of the protein except at short times.

The experimental fitting was estimated from the standard deviation calculated as follows:

$$\sigma = \frac{\sqrt{1/n\Sigma(x_i - y_i)^2}}{\sqrt{1/n\Sigma y_i^2 - (\Sigma y_i/n)^2}} \quad (16)$$

where x_i is the value of $C_{ss}(t)$ calculated from Eq. (12) and y_i is a point on the experimental curve. The result obtained with the standard deviation is 0.012 which is taken as a very good fitting of the experimental data to the proposed model.

The kinetic parameters obtained lead to conclude that the adsorption mechanism comprises the formation of a first irreversible layer that occurs in the first 8 s followed by a surface rearrangement with a possible irreversible structural change that takes approximately 15 min. This layer of the protein that undergoes changes can desorb and be detected by UV-visible spec-

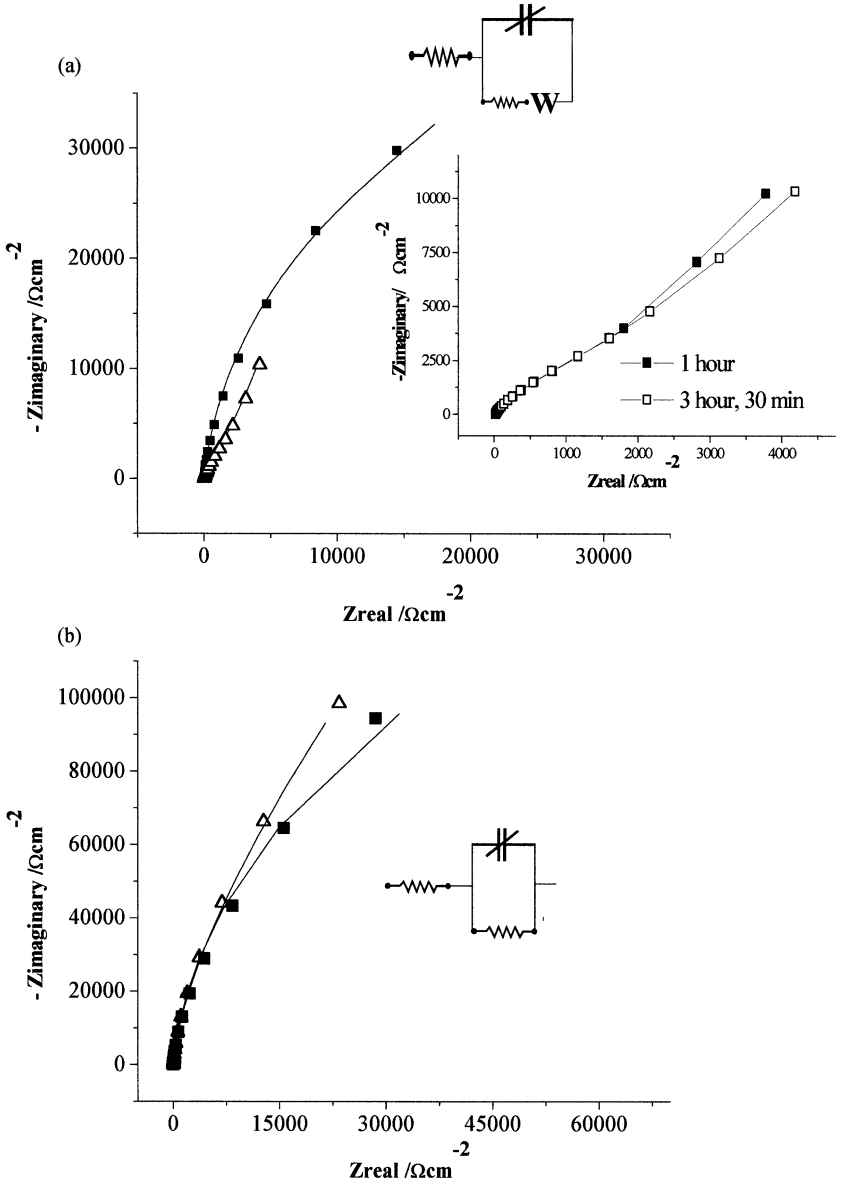

Fig. 7. Electrode impedance measured with (△) and without (■) HSA addition obtained at (a) −0.585 V and (b) 1.4 V. Fitting (—) was performed with EQUIVCRT program. The equivalent circuit shown corresponds to the best data fitting for the HSA/TiO_2 system. In the fitting procedure a pure capacity was used. The inset shows the system response for 1 h compared with the system response at longer times.

troscopy and fluorescence techniques [8]. A subsequent step is, therefore proposed where a desorption process of the modified protein is observed (k_3 in Fig. 6). This step could not be detected by pseudo-steady state impedance measurements but from the measurements performed in the steady state where a diffusion coefficient could be obtained under certain experimental conditions. This indicated that once the protein layer was formed in the steady state (at times longer than 20 min), a reversible adsorption–desorption mechanism occurs which allows detection of the protein in solution. In other words, the adsorption mechanism of HSA onto TiO_2 shows some degree of reversibility under certain experimental conditions. When the protein is adsorbed at -0.585 V, a diffusion process is observed from an impedance diagram (Fig. 7a). Under these new potential conditions, the protein would then be reversibly bound and could have a more evident adsorption–desorption mechanism. This behavior is observed even at times longer than 1 h (see inset in Fig. 7a). The observation of this fact is very important because other authors find the adsorption process of a protein essentially irreversible [14]. However, these results would be confirming the reversible character of this process and are in agreement with those of other authors that suggested that reversibly adsorbed layers are formed at times longer than in this study such as 30 min after the contact of the protein with the surface [15]. Synthetic polymers and proteins adsorbed on surfaces were detected to desorb in the presence of the macromolecule in solution by a so-called exchange mechanism [16].

3.4. Processes observed under steady state conditions

A qualitative analysis of the system is first given and then a more quantitative interpretation of the observed processes is carried out. The adsorption–desorption process of the protein on the TiO_2 in steady state depends markedly on the pH and electrode potential. The protein adsorption and the impedance spectra measurements were performed at two different potentials, -0.585 and 1.4 V. At these potentials, characteristic space charge regions are developed in the semiconductor, with different charge density, which generate a special interaction with the protein. The interplay between hydrophobic and hydrophilic forces is thought to be partially responsible for the changes in adsorption processes and these forces could be regulated also with changes of the charge that take place in the semiconductor surface. Therefore, the changes observed as a function of potential at constant pH should indicate different kinds of interactions between the protein-semiconductor interface (as well as the data taken at constant potential for different pH).

Fig. 7a shows the impedance diagrams when the potential electrode was -0.585 V. The electrode response could be related to the diffusion controlled and the activation controlled protein adsorption process. This data interpretation was first made by Lorentz et al. [17] and it is well documented in the literature and it was summarized by Sluyters et al. [18]. The interaction with the electrode is different from the one observed at 1.4 V because the diffusion process is not observed in the diagram of impedance, as it is shown in Fig. 7b. Probably, the adsorption process at this potential is more irreversible because a more positive charge at the electrode surface is developed. If the conditions that surrounded the protein are such that they destroy or decrease the magnitude of the hydrophobic interaction, then what was a reversible process is irreversible in the new environment. The behavior observed here is explained in more detail in the next section.

3.5. Impedance measurements performed at constant frequency in a potential range from -0.8 to 1.5 V

Fig. 8 shows capacity parameters as a function of pH at 18 Hz, obtained at two different potentials (0.6 and 1.4 V). It can be seen that the changes are greater when the protein and the electrode surface have opposite sign. But even when they have the same charge sign there are changes in the parameters that show the same tendency in all range of pH. This fact could be due to hydrophobic interactions, which are modified with the new protein charge. The measurements carried out up to pH 3 and 1.4 V, where the protein as well as the electrode are loaded

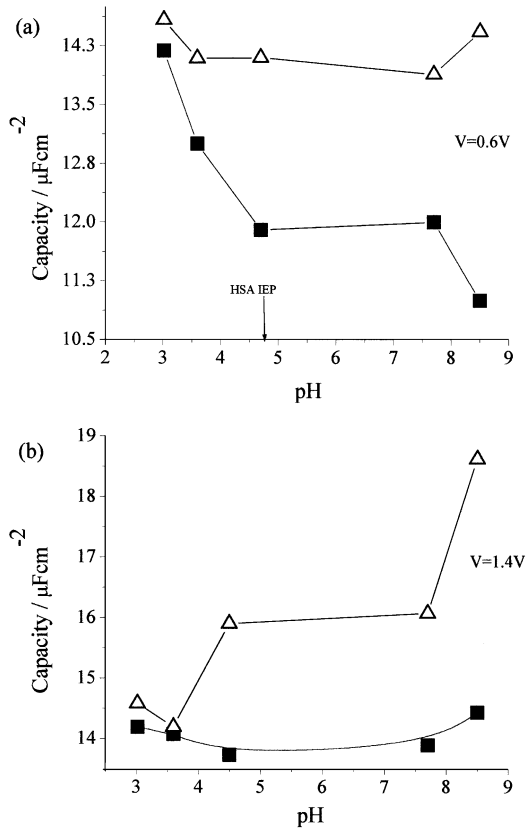

Fig. 8. Capacity vs. pH obtained in (■) 0.1 M NaCl and (△) 0.1 M NaCl + 0.1 g l^{-1} HSA at (a) 0.6 V and (b) 1.4 V, $f = 18$ Hz.

positively, show that the differences when the protein is present or absent are less than at pH 4.7 but the mechanism is the same. In the case of pH 7.7 and 1.4 V, the changes observed are greater than the ones observed at pH 4.7, so the adsorption of the protein may be enhanced by the electrostatic interactions, even more marked when the pH is far away from the IEP.

Fig. 9a shows C_T vs. potential curves for TiO_2 electrodes, in the presence and absence of the protein at pH 4.7. The greatest changes in capacity are observed as the potential becomes closer to the flat band potential V_{fb} (the potential value at which the electrostatic potential is constant, i.e. $V_{(x)} = 0$ throughout the semiconductor). This increase could be associated with changes caused by the protein at the oxide surface coinciding with the ones obtained at constant potential of −0.585 V. The curves obtained at pH 7.7 and pH 10.0 show the same change in capacity after protein addition, indicating that specific interactions prevail over electrostatic ones. The V_{fb} was calculated in an approximate way considering the Mott–Shottky model and the value obtained at pH 4.7 was −0.6 V.

3.6. Physical model of adsorption

The experimental evidence obtained under steady state conditions can be interpreted in terms of a physical model of the protein adsorption. As

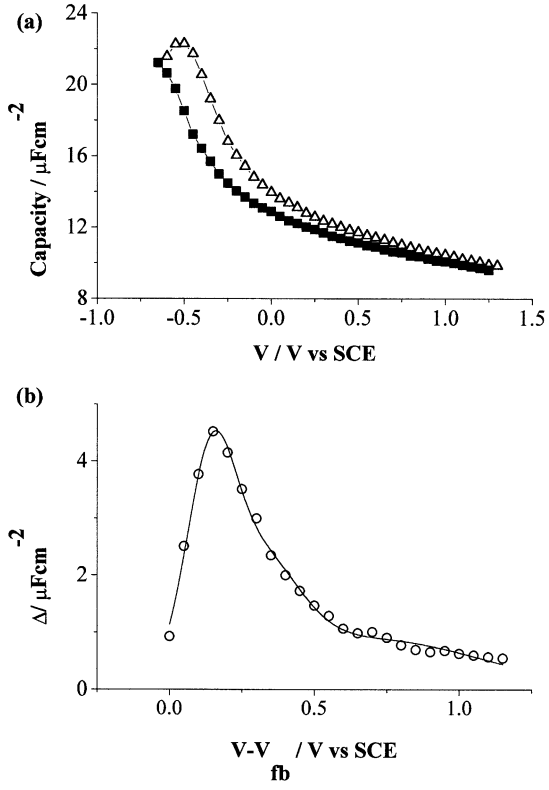

Fig. 9. (a) Capacity curves obtained at 80 Hz, pH 4.7 (△) with and (■) without protein addition. (b) Differential capacity obtained from Eq. (18) (see text). The parameters obtained from the Gaussian function corresponding to the first maximum are: $N_{ss1} = 4.1 \times 10^{18}$ cm^{-2}, $V_{t1} + V_{fb} = 0.14$ V, $\sigma_1 = 0.08$ eV. The capacity values are referred to the electrode geometric area.

it was pointed out previously, let us assume that the protein adsorption process produces mainly a change in the surface states of the oxide. These localized states can arise from titanium atoms acting as electron traps ($Ti^{4+} + e^{-}_{cb} = Ti^{3+}$), at semiconductor/electrolyte interface where the titanium atoms are partially co-ordinated to water. Experimental evidence for the existence of surface states has been reported in EPR studies of colloidal TiO_2 [19] and for impedance measurements of rutile single-crystal electrodes [20].

The experimentally accessible quantity refers to the potential drop between the electrolyte and the bulk of the semiconductor $\Delta V = V_{sc} + V_H$ where V_{sc} is the voltage across the space charge layer and V_H is the potential drop to the Helmholtz layer (see Fig 10a). The V_{sc} is given by $V_{sc} = \frac{1}{2}\frac{eN_D}{\varepsilon\varepsilon_0}W^2$ [21], where N_D is the donor concentration, W is the thickness of the space charge layer, ε is the dielectric constant of the semiconductor, ε_0 is the vacuum permittivity and e is the electron charge. When the magnitude of C_{ss} may prove to be larger than C_{sc}, it follows that $\varepsilon\varepsilon_0\bar{E}_H \approx Q_{ss}$, where $eV_H = \bar{E}_H$ is the electric field across the double layer. Then a change in the potential drop in the Helmholtz layer $dV_H = L_H d\vec{E}_H$ related with a change in the potential drop in the semiconductor dV_{sc}, is described by the ratio $-\frac{dV_H}{dV_{sc}} = -\frac{L_H}{\varepsilon_H\varepsilon_0}\frac{dQ_{ss}}{dV_{sc}} = \frac{C_{ss}}{C_H}\cdot\Delta C_{ss}$ was calculated by rearranging Eq. (2) according to:

$$\frac{1}{C_T} - \frac{1}{C_H} = \frac{1}{C_{sc} + C_{ss}} \tag{17}$$

and yield the reciprocal experimental capacities $(1/C_T)$. Considering that the Helmholtz layer remains constant and equal to 43 $\mu F/cm^2$ during the adsorption process, the mathematical operation indicated in Eq. (17) was carried out not only for the capacity values obtained in the absence of HSA but also in its presence. This procedure leads to the second term of the Eq. (17). Its reciprocal obtained under both conditions is subtracted to analyze the change in the capacity produced by the adsorption process assigned to changes in the surface states:

$$(C_{ss} + C_{sc})_{\text{with HSA}} - (C_{ss} + C_{sc})_{\text{without HSA}} = \Delta(C_{ss} + C_{sc}) \tag{18}$$

As C_{sc} and C_{ss} are in parallel, when the surface states increase considerably, it can be assumed that:

- the contribution to the C_T of the space charge region of the semiconductor is much lower than that provided by the surface state charges $C_{ss} \gg C_{sc}$. Therefore, $\Delta(C_{ss} + C_{sc}) \approx \Delta C_{ss}$; and
- the potential drop occurs mainly in the Hemholtz double layer, yielding $C_{ss} \approx \frac{Q_{ss}}{V_s}$. This variation is schematically presented in Fig. 10a,b.

Observation of the experimental dependence of the capacity ΔC_{ss} with the potential allows us to suggest that N_{ss} is a function of the energy and is no longer a constant value. Therefore, $N_{ss}(E)$ will be considered as a function of the energy described by the Gaussian distribution. The following expression yields C_{ss} as a function of potential:

$$\Delta C_{ss} = \frac{dQ_{ss}}{dV} = \frac{1}{\sqrt{2\pi}}\sum_{j=1}^{n}\frac{N_{ssj}}{\sigma_j}\cdot e^{-0.5\left(\frac{eV - eV_{tj}}{\sigma_j}\right)^2}dE \tag{19}$$

where V_{tj} is the potential that corresponds to the maximum of the function.

For the best fitting of the experimental values, three Gaussian functions were considered and the resulting curve is shown in solid line in Fig. 9b. An estimated value for the flat band potential was calculated from the Mott–Schotky plots, giving a value of -0.6 V.

According to the physical model proposed, the parameters with reasonable values are those near the flat band potential, a region where the changes associated to the protein adsorption are more important, so the values reported are $N_{ss1} = 4.1 \times 10^{18}$ cm^{-2}, $V_{t1} + V_{fb} = 0.14$ V.

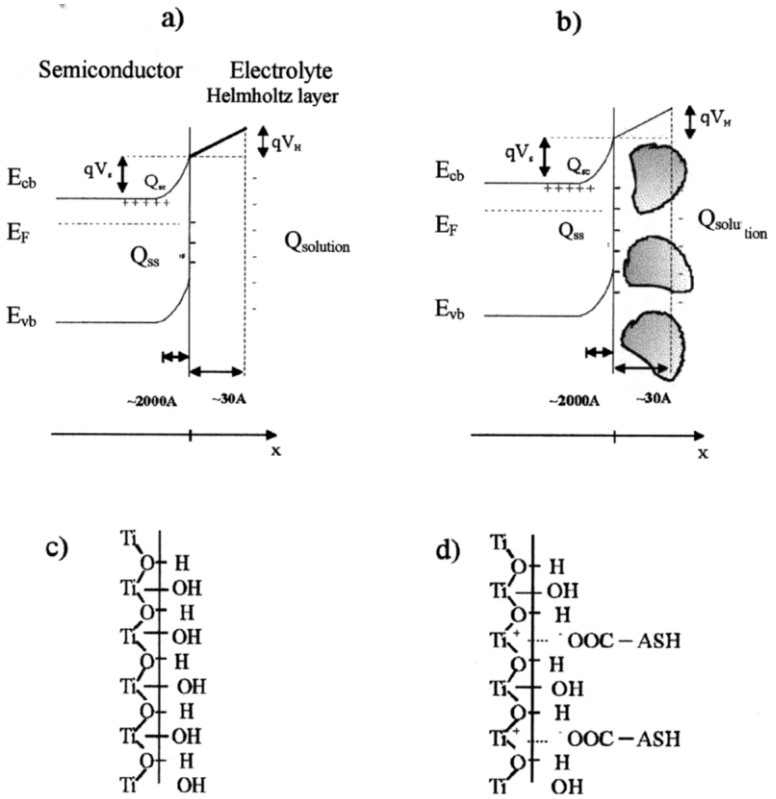

Fig. 10. Schematic representation of the system (a) when protein is absent and (b) in its presence. (c) and (d) Represent probable functional groups that may interact in the TiO_2/HSA system.

The results obtained from the application of this model are interesting. First, the appearance of several surface levels detected (at least three) when the protein layer is formed on the surface of the electrode. Second, the extrinsic nature of these states and their elevated density can indicate and/or be explained in terms of the protein–substrate interactions. Results from XPS obtained for the colloidal particles of TiO_2 with and without adsorbed protein (pH 4.7) indicate that the basic groups OH^- in the titanium surface sites are interchanged with higher probability than the acid sites, therefore, the expected reaction, schematized in Fig. 10c,d would be:

$$\mathrm{Ti(IV)^+ - {}^-OH + COO^- + H^+ \rightarrow Ti(IV)^+ - {}^-OOC + H_2O} \quad (20)$$

Schmidt et al. [22] have postulated this ligand exchange reaction for a cysteine and homocysteine interaction onto TiO_2.

4. Conclusions

Thin particulate films, which exhibit electrochemical properties similar to those of an n-type semiconductor, have been successfully studied in comparison with colloidal systems. It could be inferred that the protein adsorption under special conditions is irreversible. On the other hand, when the protein is adsorbed at -0.585 V, the impedance diagrams showed the presence of resistance and a Warburg element connected to diffusion controlled and activation controlled adsorption process.

The magnitude of the change observed depends not only on the potential at which the protein was adsorbed but also on the pH of the solution.

From these conclusions, the following points should be emphasized:

- From pseudo-steady state measurements, a two-step consecutive mechanism is postulated by interpreting the changes in capacity as produced on the surface states of the oxide due to the protein adsorption process.
- From the steady-state measurements, the changes in capacity obtained at different pH values and electrode potentials can be analyzed with a physical model which assumes a surface state distribution around a main state. Although the chemical nature of these states cannot be confirmed with this technique, an exchange mechanism is highly probable to occur due to the characteristics of the surface groups involved in the process.
- Specific HSA-TiO_2 interactions prevail over electrostatic ones as indicated by the studies in function of pH and electrode potentials.

Acknowledgements

Financial support from CONICET (Argentina) and SECyT (University of Córdoba) is gratefully acknowledged. The authors are indebted to the Alexander von Humboldt Fundation for the donation of ZANHER IM5D analyzer. We also want to acknowledge the LNLS for providing the TGM beamline and Dr R. Landers and co-workers for helpful discussions and measurements assistance. The authors also thank Miss Pompeya Falcón for language assistance.

References

[1] K. Rajeshwar, J.G. Ibanez, Electrochemical aspects of photocatalysis: applications to detoxification and disinfection scenarios J. Chem. Educ. 72 (1995) 1044–1047.

[2] S. Cosnier, C. Gondran, A. Senillou, M. Grätzel, N. Vlachopoulos, Mesoporous TiO_2 films: new catalytic electrode materials for fabricating amperometric biosensors based on oxidases Electroanalysis 9 (1997) 1387–1392.

[3] A. Sargent, T. Loi, S. Gal, O. Sadik, The electrochemistry of antibody-modified conducting polymer electrodes J. Electroanal. Chem. 470 (1999) 144–156.

[4] J.D. Andrade, Principles of Protein Adsorption, Surface and Interfacial Aspects of Biomedical Polymers, vol 2, Plenum Press, New York, 1985.

[5] O.R. Cámara, C.P. De Pauli, M.E. Vaschetto et al., Semiconducting properties of TiO_2 films thermally formed at 400°C J. Appl. Electroch. 25 (1995) 247–251.

[6] L. Avalle, E. Santos, E. Leiva, V.A. Macagno, Characterization of TiO_2 modified by Pt doping Thin Solid Films 219 (1992) 7–17.

[7] C. Natarajan, G. Nogami, Cathodic electrodeposition of nanocrystalline titanium dioxide thin films J. Electrochem. Soc. 143 (1996) 1547–1550.

[8] F.Y. Oliva, C.E. Giacomelli, C.P. De Pauli, Adsorption of human serum albumin onto TiO_2 particles, III edition, Iberoamerican Congress of Biophysics. Symposium No 266 of International Union of Biochemistry and Molecular Biology, Buenos Aires, September 1997.

[9] M. Marie de Ficquelmont-Loizos, H. Takenouti, W. Kanté, Long-time and short-time investigation of the electrode interface through electrochemical impedance measurements. Application to adsorption of human serum albumin onto glassy carbon rotating disc electrode J. Electroanal. Chem. 428 (1997) 129–140.

[10] S. Omanovic, S.G. Roscoe, Electrochemical studies of the adsorption behavior of bovine serum albumin on stainless steel Langmuir 15 (1999) 8315–8321.

[11] A. Hagfeldt, U. Björkstén, M. Grätzel, Photocapacitance of nanocrystalline oxide semiconductor films: band-edge movement in mesoporous TiO_2 electrodes during UV illumination J. Phys. Chem. 100 (1996) 8045–8048.

[12] R.M. Torresi, O.R. Cámara, C.P. De Pauli, M.C. Giordano, Influencia del cambio de pH local en la transición activa-pasiva de titanio en soluciones de sulfato a distintos pH An. Asoc. Quim. Argent. 74 (1986) 361–377.

[13] P. Bernabeu, L. Tamisier, A. De Cesare, A. Caprani, Study of the adsorption of albumin on a platinum rotating disk electrode using impedance measurements Electrochim. Acta 33 (1988) 1129–1136.

[14] A. Caprani, F. Lacour, Analysis and physical significancy of the kinetic parameters associated with albumin adsorption onto glassy carbon obtained by electrochemical impedance measurements J. Electroanal. Chem. 320 (1991) 241–258, Section: Bioelectrochemistry and Bioenergetics.

[15] K.K. Chittur, D.J. Fink, R.I. Leininger, T.B. Hutson, Fourier transform infra-red spectroscopy/attenuated total reflection studies of protein adsorption in following

system: approaches for bulk correction and composition analysis of adsorbed and bulk proteins in mixtures J. Colloid Interface Sci. 111 (1986) 419.
[16] W. Norde, C.E. Giacomelli, BSA structural changes during homomolecular exchange between the adsorbed and dissolved states J. Biotechnol. 79 (2000) 259–268.
[17] W. Lorentz, Z. Elektrochem. 62 (1958) 192.
[18] M. Sluyters-Rehbach, Impedances of electrochemical systems: terminology, nomenclature and representation. Part I: Cells with metal electrodes and liquid solutions Pure Appl. Chem. 66 (1994) 1831–1891.
[19] W. Siripala, M. Tomkiewicz, Interactions between photoinduced and dark charge transfer across n-TiO_2-aqueous electrolyte interface J. Electrochem. Soc. 129 (1982) 1240–1245.
[20] M. Tomkiewicz, The potential distribution at the TiO_2 aqueous electrolyte interface J. Electrochem. Soc.: Electrochem. Sci. Technol. 126 (1979) 1505–1510.
[21] Y.V. Pleskov, Y.Y. Gurevich, Semiconductor Photoelectrochemistry, Consultants Bureau, New York, 1986.
[22] M. Schmidt, S.G. Steinemann, XPS studies of amino acids adsorbed on titanium dioxide surfaces Fresenius J. Anal. Chem. 341 (1991) 412–415.